

Atomic Structure of the Si(111) 7×7 Surface

Peter Mark*

Department of Electrical Engineering, Princeton University, Princeton, New Jersey 08540

and

J. D. Levine and S. H. McFarlane

RCA Laboratories, Princeton, New Jersey 08540

(Received 8 April 1977)

A model for the atomic structure of the Si(111) 7×7 surface is presented on the basis of recent experimental low-energy electron diffraction (LEED) studies. The seventh-order diffracted beams are attributed to interference in the coherent scattering from the first two lattice double layers which are considered rippled with a space periodicity of seven unit cells of the ideally terminated lattice. This distortion is caused by compressive stress in the surface plane that stems from the trend toward sp^2 hybridization in these two double layers due to the presence of the free surface.

It has been known for some time from low-energy electron diffraction (LEED) studies that a well annealed, atomically ordered Si(111) surface displays seventh-order diffracted beams, suggesting a reconstructed surface superlattice with dimensions 7 times that of the bulk lattice.¹⁻⁸ However, two features of this Si(111) 7×7 LEED pattern have apparently not been recognized. The first is that the fractional order LEED patterns (comprising only the seventh-order beams; excluding the integral-order beams) display a pronounced threefold symmetry which reverses at approximately 20-V intervals of primary-beam energy. This can be seen from a comparison of the left panels of Figs. 1(a) and 1(b). These are experimental LEED patterns (negative images for clarity) of a Si(111) 7×7 surface obtained at 105 and 125 V, respectively. The experimental fractional-order LEED patterns also reveal significant changes in the pattern symmetry, short of symmetry reversal, over 5-V intervals of primary-beam energy. This is illustrated by the solid curve of Fig. 2 joining the experimental points. This curve was obtained by evaluation of the symmetry ratio $R(V)$, defined by the relation

$$R(V) = \frac{\sum_m I'(0, m, V) - \sum_m I'(0, -m, V)}{\sum_m I'(0, m, V) + \sum_m I'(0, -m, V)} \quad (1)$$

as a function of primary-beam energy (in volts) at 5-V intervals. In Eq. (1), each term is a summation of all fractional-order beam intensities (indicated by the primes) along the principal directions $+m$ or $-m$ in the (l, m) reciprocal-lattice space. Clearly, there are significant changes in the symmetry ratio in 5-V intervals, and the symmetry ratio reverses sign (changes from

+threefold to -threefold) roughly every 20 V of primary-beam energy in the range 40 to 135 V. The second major feature of the experimental LEED pattern is that the fractional-order beam intensity patterns are not the same in every ideal-lattice unit cell of reciprocal space defined by the integral-order beams. This is clearly evident from the experimental LEED patterns. The existing atomic structure models of the Si(111) 7×7 surface all consider that only atoms in the

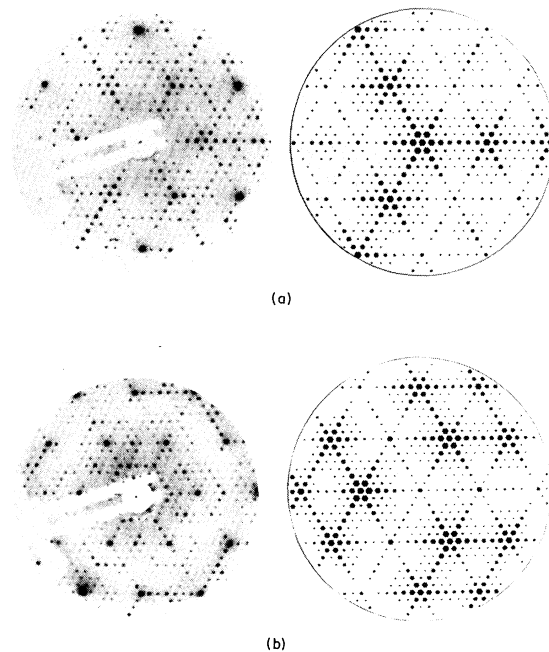


FIG. 1. Left panels, experimental LEED patterns; right panels, computed LEED patterns. (a) Primary energy, 105 V; (b) primary energy, 125 V.

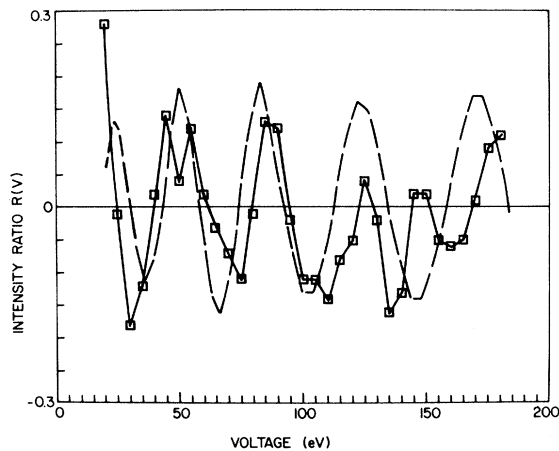


FIG. 2. Plots of the symmetry ratio $R(V)$, Eq. (1). Experimental data are the points joined by the solid curve. The dashed curve is computed from the kinematical analysis.

top atomic layer are repositioned.¹⁻⁵ It is not possible to obtain symmetry reversal as a function of primary-beam energy from such models, nor is it possible to obtain anything other than identical fractional-order beam intensity patterns in every ideal-lattice unit cell of reciprocal space.⁹ Thus, the existing surface-structure models are inadequate in accounting for the major features of the experimental data.

The proposed new model of the surface deformation of Si(111) 7×7 is illustrated in Fig. 3 which is an elevation of the top three double layers in the $[11\bar{2}]$ direction. The model considers the surface to have a ripplelike deformation of at least the top two double layers. There is a trend toward sp^2 hybridization in the double layers near the surface driven by the dangling bonds at the free surface when it is formed. This tendency to transform the double layers into graphite-like layers generates a compressive stress in the surface plane to which the ripple distortion is attributed.⁹ The rehybridization of the top double layer, which is most strongly affected, also causes the weakening of the back bonds of the first double layer to the second double layer, and so on into the crystal. However, the effect, and the associated distortion, is sufficiently small that the experimental observations embodied in Eq. (1) can be adequately reproduced by considering the distortions as perturbations in the evaluation of the lattice scattering factor, and by considering distortions only of the first

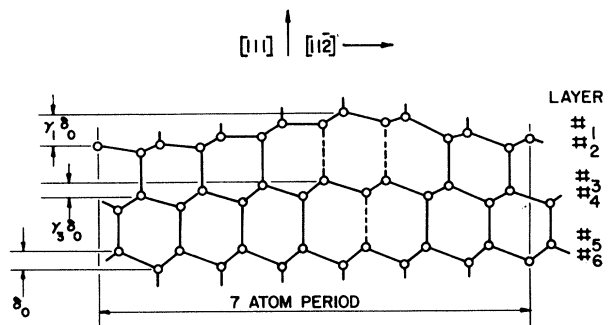


FIG. 3. Schematic representation of the Si(111) surface region of the first three double layers along a $[11\bar{2}]$ cut illustrating the rippled deformation responsible for the 7×7 LEED pattern. The ripple amplitudes are shown greatly exaggerated for clarity. These amplitudes are treated as perturbations in the analysis. The dashed bonds simulate bonds "weakened" by rehybridization.

two double layers and neglecting the deformations of succeeding double layers.

The objective of the model is to reproduce the basic features of the symmetry variations of the fractional-order LEED patterns with primary-beam energy, not the detailed computation of the beam-intensity-primary-energy dependence of every fractional-order beam. Following the procedures established by Duke and Tucker,¹⁰ it suffices to compute the kinematical Bragg envelopes of the normal-incidence, fractional-order beam intensity profiles.¹¹ The lattice scattering factor for an individual LEED beam in this kinematical analysis is given by

$$f = \sum_{n=1}^{\infty} \sum_{\vec{r}_n}^{49} \exp i(\vec{k}_{\parallel} \cdot \vec{r}_n) \exp i[k_{\perp} Z_n(\vec{r}_n)], \quad (2)$$

where n is a layer index and where (\vec{r}_n) and $Z_n(\vec{r}_n)$ are the lateral and depth coordinates, respectively, that locate the 49 atoms in the distorted unit cell. The proposed distortion dictates that $Z_n(\vec{r}_n)$ be a sevenfold periodic function of \vec{r}_n . The lateral wave vector is \vec{k}_{\parallel} and the normal component of the wave vector is $k_{\perp} = 2\pi[150(V + V_0)]^{1/2}(1 + \cos\theta)$ where θ is the beam exit angle relative to the surface normal and V_0 is the inner potential which has been given the value 10 V to achieve best agreement between experiment and the computed results.

As only the fractional-order beam symmetry variations are of interest, Eq. (2) can be written

as

$$f(l, m) = ik_{\perp} \delta_0 \left[\gamma_1 \sum_{\vec{r}_n}^{98} F(\vec{r}_n) \exp i(\vec{k}_{\parallel} \cdot \vec{r}_n) + \gamma_3 \exp i(k_{\perp} D) \sum_{\vec{r}_n}^{98} F(\vec{r}_n') \exp i(\vec{k}_{\parallel} \cdot \vec{r}_n') \right], \quad (3)$$

where the following approximations and simplification have been incorporated. First, the depth coordinate is expressed by a sum so that $Z_n(\vec{r}_n) = \zeta_n + \gamma_n \delta_0 F(\vec{r}_n)$, where $\delta_0 = 0.78 \text{ \AA}$, the double-layer thickness; $n = 1, 2, 3, \dots$; $\zeta_n = 0, \frac{1}{4}D, D, 1\frac{1}{4}D, \dots$, where $D = 4\delta_0$ (the spacing between double layers); $\gamma_n \delta_0$ is the ripple amplitude of the n th layer; $F(\vec{r}_n)$ is the common ripple shape factor. Second, the ripple amplitudes $\gamma_n \delta_0$ are considered small for all layers, sufficiently so that they are treated as perturbations. Further, as the ripple amplitude must decrease with increasing n , it is assumed that $\gamma_n (n > 4) = 0$. That is, the ripple distortion of the first two double layers only are retained. Third, for the 7×7 lattice, $\vec{k}_{\parallel} \cdot \vec{r}_n = (2\pi/7) \times (ls_n + mt_n)$, where l, m, s_n , and t_n are integers, where the fractional-order beams are defined by l and m not multiples of 7 and where

$$\sum_{\vec{r}_n}^{98} \exp i(\vec{k}_{\parallel} \cdot \vec{r}_n) = 0$$

for all fractional-order beams. Finally, it is assumed, because of the rehybridization trend in the distorted top two double layers, that their

thicknesses have been diminished sufficiently compared with D that each of these double layers can be well approximated mathematically by a single layer. That is, $\zeta_1 = \zeta_2$, $\zeta_3 = \zeta_4$; $\gamma_1 = \gamma_2$, $\gamma_3 = \gamma_4$, so that each of these double layers has (mathematically) a nearly graphitelike Si structure. The vectors \vec{r} and \vec{r}' locate the atoms in the first and second graphitelike layers and are related by the expression

$$F(\vec{r}') = \frac{1}{3} \sum_{n=1}^3 F(\vec{r}_n),$$

where the sum extends over the three nearest neighbors on the other graphitelike layer.¹² These simplifications allow the analysis to remain analytically tractable without at the same time obscuring the physical content, namely, the computation of the primary-beam energy dependence of the symmetry properties of the fractional-order LEED patterns.

The intensity $I(l, m, V)$ of each fractional-order LEED beam derived from the kinematical interference between the two rippled, graphitelike layers is given by $f^* f$ from Eq. (3), and can be written as

$$I(l, m, V) = (k_{\perp} \delta_0 \gamma_1)^2 (1 + \cos \theta)^2 G^2(l, m) |T(l, m, \gamma, V)|^2, \quad (4)$$

where $\gamma = \frac{1}{3} \gamma_3 / \gamma_1$ is the amplitude coefficient ratio of the top and second graphitelike layers and

$$G(l, m) = \sum_{\vec{r}}^{98} F(\vec{r}) \exp i(\vec{k}_{\parallel} \cdot \vec{r}).$$

Since the function $F(\vec{r})$ is unknown, $G(l, m)$ cannot be computed. However, as this term is six-fold symmetric and independent of the primary-beam energy, it does not contribute to the dependencies which are the subject of this Letter. In fact, this term merely contributes a constant magnitude to the fractional-order beam intensities, repeats in every ideal-lattice unit cell of reciprocal space, and in no way affects the symmetry ratio $R(V)$. The important term in this discussion is the translational function $T(l, m, \gamma, V)$ which is threefold symmetric, depends on the primary-beam energy, and repeats only in every third ideal-lattice unit cell in the reciprocal space.

The computed LEED patterns in the right panels of Figs. 1(a) and 1(b) were computer-generated from Eq. (4) with the following "best fit" inputs. The amplitude coefficient ratio $\gamma = -0.1$, and $G^2(0, m) = G^2(0, -m) = 100$ for the fractional-order beams on a principal reciprocal-space coordinate direction while for all other fractional-order beams $G^2(l, m) = 9$. The computed fractional-order beam intensities were then normalized by determining the maximum and minimum beam intensities by a search routine and subsequently assigning the value zero to the minimum intensity and unity to the maximum intensity. The graphic display prints out hexagonal "spots" whose sizes scale with the beam intensities.

The symmetry ratio Eq. (1) was also evaluated for the computed beam intensities in exactly the same way as it was for the experimental fraction-

al-order LEED patterns: Only the fractional-order beams contribute to each sum in the ratio. The computed ratio is also plotted on Fig. 2 as the dashed curve. Clearly, there is very good correspondence between the computed and experimental curves in the voltage range 40 to 135 V. Both curves display a periodic symmetry reversal with the crossover points (points of sixfold symmetry) spaced at intervals of approximately 20 V. In addition, the computed fractional-order LEED patterns of Fig. 1 do not have the same fractional-order beam intensity distribution within each ideal-lattice unit cell of reciprocal space, in agreement with the experimental LEED patterns. Neither of these correspondences can be achieved solely with the existing surface-defect (i.e., vacancy,¹⁻³ adatom,⁵ and stacking fault⁴) models. It is not clear at this writing whether the proposed rippled surface and any of the existing proposed surface-defect structures can coexist and still provide the observed seventh-order diffraction beams and their symmetry properties. However, regardless of such possible coexistence, it is clear that the proposed ripple surface deformation is a necessary *and* sufficient condition for the observation of the experimental data presented here.

The experimental symmetry reversals evident in Fig. 2 become inconsistent with the computed reversals below about 40 V and above about 135 V of primary-beam energy. This is attributed to the energy dependence of the electron inelastic scattering length on electron energy: $\lambda \approx 0.7\sqrt{V}$ (λ in angstroms, V in volts) for $V \geq 10$ V. Consequently, below about 40 V, the primary electron beam penetrates predominately only the top layer (the top graphitelike layer in the mathematical approximation). Hence, at these low voltages, there is no interference effect between the first two double layers and the fractional-order LEED

pattern should exhibit nearly sixfold symmetry, independent of the primary voltage. Alternately, above about 140 V, the primary beam begins to penetrate three double layers and the fractional-order LEED pattern symmetry behavior should show departures from computed symmetry effects derived from two-double-layer models. These details and others pertaining to the interpretation of fractional order Si(111) 7×7 LEED patterns are given elsewhere.¹²

We wish to thank M. Bonn and G. Cisneros for help with the experiments.

*Supported by Office of Naval Research (Contract No. N00014-75-C-0394), Army Research Office (Contract No. DAHC-04-74-G0133), and National Science Foundation (Contract No. GK 38575).

¹J. J. Lander and J. Morrison, *J. Appl. Phys.* **34**, 1403 (1963).

²J. C. Phillips, *Surf. Sci.* **40**, 459 (1973).

³K. C. Pandey and J. C. Phillips, *Phys. Rev. Lett.* **34**, 1450 (1975).

⁴N. R. Hansen and D. Haneman, *Surf. Sci.* **2**, 566 (1964).

⁵W. A. Harrison, *Surf. Sci.* **55**, 1 (1976).

⁶J. V. Florio and W. D. Robertson, *Surf. Sci.* **22**, 459 (1970).

⁷H. Iback and J. E. Rowe, *Surf. Sci.* **43**, 481 (1974).

⁸G. Margaritondo, S. B. Christian, and J. E. Rowe, *J. Vac. Sci. Technol.* **13**, 329 (1976).

⁹J. D. Levine, P. Mark, and S. H. McFarlane, to be published.

¹⁰C. W. Tucker and C. B. Duke, *Surf. Sci.* **23**, 411 (1970), and *J. Vac. Sci. Technol.* **8**, 5 (1971).

¹¹A complete dynamical scattering analysis of the proposed surface structure is impossible with present computer capabilities because of the large number of atoms in the surface unit cell.

¹²J. D. Levine, P. Mark, and S. H. McFarlane, to be published.

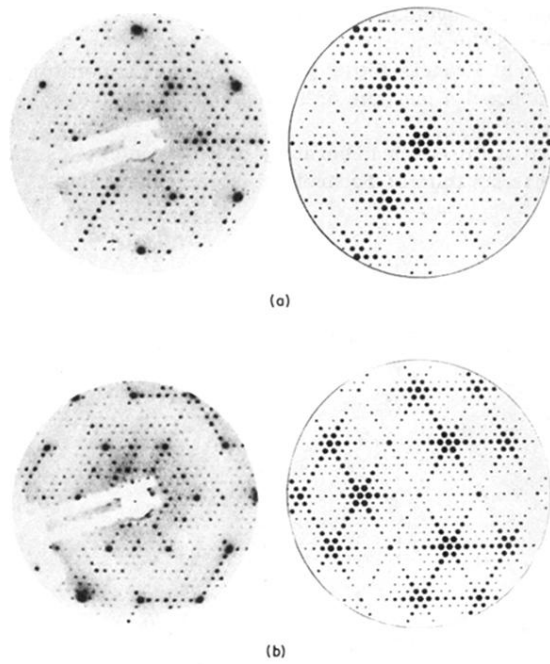


FIG. 1. Left panels, experimental LEED patterns; right panels, computed LEED patterns. (a) Primary energy, 105 V; (b) primary energy, 125 V.